

1 **The effect of *SLCO1B1* polymorphisms on the pharmacokinetics of**
2 **rifabutin in African HIV-infected patients with tuberculosis**

3

4 Stefanie Hennig^{1*}, Suhashni Naiker^{2*}, Tarylee Reddy³, Deirdre Egan⁴, Tracy
5 Kellerman⁵, Lubbe Wiesner⁵, Andrew Owen⁴, Helen McIlleron⁵ and Alexander Pym^{2,}

6 ^{6*}

7

8 ¹ School of Pharmacy, The University of Queensland, Australia;

9 ²TB Research Unit, Medical Research Council, Durban, South Africa;

10 ³Biostatistics Unit, Medical Research Council, Durban, South Africa;

11 ⁴Department of Molecular and Clinical Pharmacology, University of Liverpool,
12 United Kingdom;

13 ⁵Division of Clinical Pharmacology, Department of Medicine, University of Cape
14 Town, Cape Town, South Africa;

15 ⁶KwaZulu-Natal Research Institute for Tuberculosis & HIV (K-RITH), Nelson
16 Mandela School of Medicine, Durban, South Africa.

17

18 *These authors contributed equally to the manuscript

19 *Corresponding author: Alexander Pym, KwaZulu-Natal Research Institute for Tuberculosis & HIV
20 (K-RITH), Nelson R. Mandela School of Medicine, K-RITH Tower Building, 719 Umbilo Road,
21 Durban alex.pym@k-rith.org Tel +27 31 260 4991 |Direct Tel +27 31 260 4979 |Fax +27 31 260
22 4203 |Cell +27 765249773.

23

24 Keywords: rifabutin, 25-desacetyl rifabutin, OATP1B1 transporter, pharmacogenomics,
25 pharmacokinetics

26

27 Running Title: *SLCO1B1* polymorphisms and pharmacokinetics of rifabutin

28 ***Abstract***

29 Rifabutin used in HIV-infected tuberculosis shows highly variable drug exposure
30 complicating dosing. Effects of *SLCO1B1* polymorphisms on rifabutin
31 pharmacokinetic were investigated in 35 African HIV-infected tuberculosis patients
32 after multiple dosing. Nonlinear mixed-effects modelling found influential covariates
33 on the pharmacokinetics were weight, sex and a 30% increased bioavailability
34 amongst heterozygous carriers of *SLCO1B1* rs1104581 (previously associated with
35 low rifampicin concentrations). Larger studies are needed to understand the complex
36 interactions of host genetics in HIV-infected tuberculosis patients.

37

38 ***Introduction***

39 Rifabutin is an alternative rifamycin for tuberculosis treatment. It is also used to treat
40 other mycobacterial infections and to prevent *Mycobacterium avium* complex in
41 patients with AIDS. Unlike rifampicin, rifabutin does not reduce concentrations of
42 concomitantly administered protease inhibitors (PI) significantly (1). The
43 pharmacokinetics of rifabutin are highly variable. (2-4) As a CYP3A4 substrate
44 rifabutin is subject to drug interaction with CYP3A4 inhibitors, such as PIs and
45 increases the exposure can result in an increased risk for adverse effects, particularly
46 uveitis. Toxicity including uveitis, neutropenia and hepatotoxicity are a concern with
47 high exposures (5). Conversely, low rifabutin exposures are associated with relapse
48 and acquired rifamycin resistance (6). While therapeutic drug monitoring is advocated
49 it is seldom available (5). Although a lack of suitable formulations and cost limit the
50 widespread use of the drug in resource-constrained settings, its use is increasing in
51 combination with PIs as ART programs mature and more patients are started on 2nd
52 line PI-based regimens.

53

54 In a process subject to autoinduction, arylacetamide deacetylase converts rifabutin to
55 the active primary metabolite, 25-desacetyl rifabutin, which is in turn metabolized by
56 CYP3A4 (7, 8). Organic anion transporting polypeptide 1B1 (OATP1B1) mediates
57 hepatocellular influx of diverse xenobiotics prior to excretion in bile (9). Functional
58 single nucleotide polymorphisms (SNPs) in *SLCO1B1*, the gene encoding OATP1B1
59 have been associated with significant alterations in drug pharmacokinetics. *SLCO1B1*
60 rs4149032 and rs11045819 have been associated with lower rifampicin and lopinavir
61 concentrations (10-12), while the rs4149056 SNP is associated with higher
62 concentrations of lopinavir and other drugs including statins (13, 14). The *SLCO1B1*

63 rs2306283 variant is associated with increased OATP1B1 expression (15). The allele
64 frequencies of *SLCO1B1* vary markedly between different populations (16). We
65 recently showed that *SLCO1B1* rs4149032 is carried by 70% of South Africans in
66 whom it predicted reduced rifampicin concentrations (10). Since little is known about
67 pharmacogenomic determinants of rifabutin exposure, we investigated the frequencies
68 of *SLCO1B1* SNPs rs4149032, rs11045819, rs4149056 and rs2306283, and their
69 effects along with other covariate factors, on the pharmacokinetics of rifabutin in
70 HIV-infected patients with tuberculosis prior to initiation of ART.

71 **Methods**

72 The pharmacokinetics and safety of rifabutin was investigated in 44 patients with
73 HIV-associated tuberculosis as part of the ANRS 12150a trial (ClinicalTrials.gov
74 registration no. NCT00640887). After 6 weeks on standard antituberculosis treatment,
75 patients were switched from rifampicin to rifabutin 300 mg daily for the last 2 weeks
76 of the intensive phase (with standard isoniazid doses, pyrazinamide and ethambutol)
77 and for the first 2 weeks of the continuation phase (with standard isoniazid doses). All
78 study participants had microbiologically confirmed pulmonary tuberculosis, HIV
79 infection (CD4 lymphocyte count 50-200 cells/mm³), weight ≥ 50 kg or BMI > 18 , a
80 Karnofsky score $Q \geq 80\%$ and no grade 3 or 4 clinical or laboratory findings according
81 to DMID tables (17).

82 After 4 weeks on rifabutin 300 mg daily without ART, patients were admitted for
83 pharmacokinetic evaluation. Following an overnight fast, blood samples were drawn
84 immediately before dosing and at 2, 3, 4, 5, 6, 8, 12 and 24 h after dosing. A standard
85 hospital breakfast (oats with 2 slices of toast and tea) was served >2 hours after
86 dosing. Samples were placed on ice, until the plasma was separated and stored
87 at -80°C , within 30 minutes of sampling. Forty-two patients provided additional

88 written informed consent for the pharmacogenetic testing. A whole blood sample was
89 collected and stored for genetic analysis.

90 Rifabutin and 25-desacetyl rifabutin were assayed by LC/MS/MS as described
91 previously (18). For both analytes, inter-batch accuracy (%Nom) was 99.1-109.0%
92 and precision (%CV) was <9.2% at low, medium and high QC levels. The calibration
93 ranges were 3.91-1000 ng/ml and 0.780-200 ng/ml for rifabutin and 25-desacetyl
94 rifabutin respectively.

95 Genotyping for *SLCO1B1* rs4149032, rs2306283, rs4149056 and rs11045819 was
96 performed using real-time PCR allelic discrimination by standard methodology
97 (Supplementary material).

98 The pharmacokinetics of rifabutin and 25-desacetyl rifabutin were described using a
99 population nonlinear mixed-effects model in NONMEM (19) (Supplementary
100 material). Structural base model building was followed by covariate model
101 development. Firstly, the influence of patient's weight and lean body weight,
102 respectively, were investigated on all apparent clearance and apparent volume
103 parameters of rifabutin using allometric scaling *a priori* (20). Influence of age, sex
104 and the SNPs (*SLCO1B1* rs414903, rs2306283 and rs11045819 respectively) on
105 model parameters were then each investigated in a stepwise fashion. As only 1 subject
106 carried rs4149056, this SNP was not included in the covariate analysis.

107 The final model was used in Monte Carlo simulations (500 simulation of the original
108 study design) to estimate area under the concentration–time curve (AUC) over the
109 24h dosing interval (AUC₀₋₂₄) for rifabutin, and metabolite (AUCM₀₋₂₄) and
110 investigate the relevance of dose adjustment based on significant covariate factors
111 Differences in AUC measures between males and females and rs11045819 carriers

112 and non-carriers were evaluated using the Mann-Whitney Wilcoxon test (Rstudio
113 Version 0.98.501).

114 **Results**

115 Forty-four patients (61% males) with mean (sd) weight, height, body mass index, age
116 and CD4 lymphocyte count of 60.7 (8.7) kg, 159.6 (7.7) cm, 22.8 (3.3) kg/m²,
117 32.7(5.9) years and 126.1(44.0) cells/mm³ respectively, contributed 780
118 pharmacokinetic observations. The Karnovsky score was 100 in all patients. All
119 patients were of Black African ethnicity. Genetic samples were not available for 7 of
120 these patients and in a further 2 patients analysis of rs4149032 was unsuccessful
121 (Table 1).

122 A 2-compartment model with first-order absorption after a lag-time and first-order
123 elimination from the central compartment best described rifabutin pharmacokinetics.
124 Simultaneously, metabolism to the 25-desacetyl rifabutin metabolite was modeled via
125 a first order process. The metabolite model was also best described by 2-
126 compartments with linear elimination from the central compartment (Fig. S1 in the
127 supplemental material). The final population parameter estimates are shown in Table
128 2. Body weight allometrically scaled (20) on rifabutin apparent clearances (from the
129 central compartment; inter-compartmental clearance; clearance to the metabolite) and
130 apparent central and peripheral volume of distribution improved the model (change in
131 objective function value (Δ OFV)=-6.79). Males had a 1.84 times higher central
132 volume of distribution for rifabutin than females (Δ OFV=-20.9), accounting for a
133 31.3% reduction in between subject variability (BSV) on V/F. After weight and
134 gender were included in the model the effects of rs4149032, rs2306283 and
135 rs11045819 were evaluated on bioavailability (F; with the nominal population value
136 of 1), apparent oral metabolism clearance to des-rifabutin (CL_e/F), rifabutin

137 intercompartmental clearance (Q), apparent oral clearance of des-rifabutin (CL_m/F),
138 and volumes of distribution of the parent and metabolite. The rs11045819 SNP was
139 associated with a 30% increase in F ($\Delta OFV=-6.5$) and reduced BSV on F by 8.9%.

140

141 Although the drop in OFV was significant, the changes visible in the visual predictive
142 check (VPC) were minor. Inclusion of other SNP effects on the pharmacokinetic
143 parameters did not statistically improve the model fit. The VPC (Fig. S2 in the
144 supplemental material) displayed good model predictability and other goodness-of-fit
145 plots (Fig. S3 in the supplemental material) further validated the final model. The
146 influence of all covariate effects on overall exposures (AUC_{0-24} , $AUCM_{0-24}$) of
147 rifabutin and the metabolite for subpopulations can be found in supplemental material
148 Table S1.

149 ***Discussion***

150 We investigated the effect of *SLCO1B1* polymorphisms, weight and sex on rifabutin
151 concentrations in an African population with HIV-associated tuberculosis. We found
152 that rifabutin bioavailability was 30% higher amongst heterozygous carriers of the
153 *SLCO1B1* rs11045819 polymorphism compared to non-carriers. The effect on
154 bioavailability was significant within the model, resulting in a significant difference
155 between the estimated exposures for carriers and non-carriers (Supplemental material
156 Table 1). Larger studies are needed to confirm the effect and characterize its effect on
157 rifabutin exposure in patients. Interestingly, prior studies associated this
158 polymorphism with reduced rifampicin and lopinavir concentrations (11, 12).
159 *SLCO1B1* rs4149032 was also associated with reduced rifampin exposure in South
160 African tuberculosis patients (10). We did not find this polymorphism to affect
161 rifabutin exposure; however our study included insufficient carriers of this

162 polymorphism to exclude an association. While rs4149056 is more frequent in Asian
163 and Caucasian populations, the low frequency of this SNP in our study (Table 1) is
164 consistent with the reported population frequency (0.7-11.5%) in sub-Saharan Africa
165 (21).

166 Relationships between drug concentrations and OATP1B1 variants are complex.
167 SNPs may be associated with altered OATP1B1 expression, or loss of function (12-
168 14). Moreover, rifampicin inhibits OATP1B1 (13), while rifampicin but not rifabutin
169 induced OATP1B1 mRNA expression in hepatocytes incubated with 0.5, 5, or 10 μ M
170 concentrations of the drugs (9). A better understanding of these complex factors is
171 necessary to explain the disparate effects of *SLCO1B1* rs1104581 on rifampicin and
172 rifabutin. As lopinavir is a substrate and inhibitor of OATP1B1 (22) and, like
173 rifabutin and 25-desacetyl rifabutin, is a CYP3A4 substrate, further studies are needed
174 to evaluate the impact of genetic variants on rifabutin pharmacokinetic, safety and
175 efficacy with concomitant lopinavir/ritonavir.

176 A further finding in this study is the effect of gender on the distribution of rifabutin
177 after adjusting for weight. A possible explanation for the importance of both weight
178 and gender effects could be differences in body composition between men and
179 women (23, 24). However, allometric scaling using lean body weight and total body
180 weight, respectively, were tested in the model and total body weight was superior.

181 In conclusion, we explored factors contributing to wide variability in rifabutin
182 exposures in HIV-infected patients with tuberculosis. The *SLCO1B1* rs1104581
183 polymorphism, weight and gender appear to play important roles, however, larger
184 studies are needed to confirm these effects before they could be used to optimize
185 dosing.

186 **Tables**

187 Table 1. Allele Frequencies

Allele	<i>Numbers of patients with the polymorphism (Number of patients with missing data regarding the polymorphism)</i>
<i>SLCO1B1</i> rs4149032	CC=5, CT=11, TT=17, (9)
<i>SLCO1B1</i> rs2306283	AG=8, GG=27, (7)
<i>SLCO1B1</i> rs4149056	CC=34, CT=1, (7)
<i>SLCO1B1</i> rs11045819	AC=5, CC=30, (7)

188 **Table 2:** Population pharmacokinetic parameter estimates of the base model and the final model for rifabutin and des-rifabutin

	<i>Final model</i>		<i>Bootstrap results</i>		<i>Base model</i>	
			<i>Median (RSE %)</i>			
OFV	-1413.8		-1432.5 (7.8)		-1386.4	
<i>Rifabutin parameters</i>	<i>BSV (%)</i>		<i>BSV (%)</i>		<i>BSV (%)</i>	
Clearance Cl/F (L/h/70 kg)	116.5	12.0	108.2 (18.2)	11.6 (126.8)	114.3	16.0
Central volume of distribution V/F (L/70kg)	117.8	49.0	121.7.6 (53.8)	52.3 (54.0)	148.8	58.0
Absorption rate constant k_a (1/h)	0.24	23.9	0.22 (47.7)	24.9 (81.5)	0.21	26.0
Lag time (h)	1.6	24.7	1.7 (8.6)	20.2 (69.2)	1.5	25.0
Bioavailability F (Fixed)	1	33.0	1	28.3 (35.2)	1	34.0
Q/F (L/h/70 kg)	123.8		121.9 (23.0)		111.9	
V_{per}/F (L/70kg)	4897.8		4904.8 (116.1)		4663.8	
Cl_e/F (metabolism of RBN to des-RBN)	21.2		21.2 (52.5)		18.8	
<i>des-Rifabutin parameters</i>						
Cl_m/F (L/h)	196.7	30.0	200.4 (53.8)	27.5 (20.5)	174.1	30.0

V_m/F (L)	3.9	3.8 (77.8)	3.5
Q_m/F (L/h) (Fixed)	0.15		0.15
V_{m-per}/F (L) (Fixed)	536.8		536.8
Residual error			
Proportional error rifabutin (%)	34.6	33.8 (18.3)	34.6
Proportional error des-rifabutin (%)	34.6	34.2 (28.6)	33.2
Additive error rifabutin (ng/ml)	14.0	12.8 (13.9)	14.4
Additive error des-rifabutin (ng/ml)	1.2	1.3 (24.7)	1.17
<i>Covariate effects</i>			
Increase of V/F for males (factor)	1.8	1.3 (33.3)	
Increase in bioavailability F (%) for rs11045819 genotype	30.4	39.7 (71.6)	

189

190 Cl -clearance, V = volume of distribution for rifabutin in the central compartment, V_{per} - volume of distribution for rifabutin in the peripheral compartment, ka -

191 first order absorption rate constant, F - bioavailability, Q - intercompartmental clearance for rifabutin, Cl_e - clearance of rifabutin to des-rifabutin, BSV –

192 between subject variability, Cl_m - clearance of des-rifabutin, V_m - volume of distribution for des-rifabutin in the central compartment, V_{m-per} - volume of
193 distribution for des-rifabutin in the peripheral compartment, the base model included weight allometrically scaled on CL/F , V/F , Q/F and V_{per}/F
194

Acknowledgements

We wish to thank the following: Roxana Rustomjee for support in carrying out the study and to the patients and their families who participated in the study.

Transparency declarations

None of the authors have any conflict of interest to declare.

Funding

This study was supported by French National Agency for Research on AIDS and Viral Hepatitis (ANRS). HM is supported in part by the National Research Foundation of South Africa (Grant Number 90729). Pfizer South Africa supplied the rifabutin. Pharmacokinetic analysis reported in this publication was supported by the National Institute of Allergy and Infectious Diseases of the National Institutes of Health under Award Number UM1 AI068634, UM1 AI068636 and UM1 AI106701. The content is solely the responsibility of the authors and does not necessarily represent the official views of the National Institutes of Health. The funders had no role in study design, data collection and analysis, decision to publish, or preparation of the manuscript.

References

1. **Polk RE, Brophy DF, Israel DS, Patron R, Sadler BM, Chittick GE, Symonds WT, Lou Y, Kristoff D, Stein DS.** 2001. Pharmacokinetic Interaction between amprenavir and rifabutin or rifampin in healthy males. *Antimicrob Agents Chemother* **45**:502-508.
2. **Lan NT, Thu NT, Barrail-Tran A, Duc NH, Lan NN, Laureillard D, Lien TT, Borand L, Quillet C, Connolly C, Lagarde D, Pym A, Lienhardt C, Dung NH, Taburet AM, Harries AD.** 2014. Randomised pharmacokinetic trial of rifabutin with lopinavir/ritonavir-antiretroviral therapy in patients with HIV-associated tuberculosis in Vietnam. *PLoS One* **9**:e84866.

3. **Gatti G, Papa P, Torre D, Andreoni M, Poggio A, Bassetti M, Marone P.** 1998. Population pharmacokinetics of rifabutin in human immunodeficiency virus-infected patients. *Antimicrob Agents Chemother* **42**:2017-2023.
4. **Naiker S, Connolly C, Wiesner L, Kellerman T, Reddy T, Harries A, McIlleron H, Lienhardt C, Pym A.** 2014. Randomized pharmacokinetic evaluation of different rifabutin doses in African HIV- infected tuberculosis patients on lopinavir/ritonavir-based antiretroviral therapy. *BMC Pharmacol Toxicol* **15**:61.
5. **CDC.** 2013. Managing Drug Interactions in the Treatment of HIV-Related Tuberculosis [online]. Available from URL: http://www.cdc.gov/tb/TB_HIV_Drugs/default.htm (last accessed 30 July 2014).
6. **Weiner M, Benator D, Peloquin CA, Burman W, Vernon A, Engle M, Khan A, Zhao Z.** 2005. Evaluation of the drug interaction between rifabutin and efavirenz in patients with HIV infection and tuberculosis. *Clin Infect Dis* **41**:1343-1349.
7. **Trapnell CB, Jamis-Dow C, Klecker RW, Collins JM.** 1997. Metabolism of rifabutin and its 25-desacetyl metabolite, LM565, by human liver microsomes and recombinant human cytochrome P-450 3A4: relevance to clinical interaction with fluconazole. *Antimicrob Agents Chemother* **41**:924-926.
8. **Nakajima A, Fukami T, Kobayashi Y, Watanabe A, Nakajima M, Yokoi T.** 2011. Human arylacetamide deacetylase is responsible for deacetylation of rifamycins: rifampicin, rifabutin, and rifapentine. *Biochem Pharmacol* **82**:1747-1756.
9. **Williamson B, Soars AC, Owen A, White P, Riley RJ, Soars MG.** 2013. Dissecting the relative contribution of OATP1B1-mediated uptake of xenobiotics into human hepatocytes using siRNA. *Xenobiotica* **43**:920-931.
10. **Chigutsa E, Visser ME, Swart EC, Denti P, Pushpakom S, Egan D, Holford NH, Smith PJ, Maartens G, Owen A, McIlleron H.** 2011. The SLCO1B1 rs4149032 polymorphism is highly prevalent in South Africans and is associated with reduced rifampin concentrations: dosing implications. *Antimicrob Agents Chemother* **55**:4122-4127.
11. **Weiner M, Peloquin C, Burman W, Luo CC, Engle M, Prihoda TJ, Mac Kenzie WR, Bliven-Sizemore E, Johnson JL, Vernon A.** 2010. Effects of tuberculosis, race, and human gene SLCO1B1 polymorphisms on rifampin concentrations. *Antimicrob Agents Chemother* **54**:4192-4200.
12. **Lubomirov R, di Iulio J, Fayet A, Colombo S, Martinez R, Marzolini C, Furrer H, Vernazza P, Calmy A, Cavassini M, Ledergerber B, Rentsch K, Descombes P, Buclin T, Decosterd LA, Csajka C, Telenti A, Swiss HIVCS.** 2010. ADME pharmacogenetics: investigation of the pharmacokinetics of the antiretroviral agent lopinavir coformulated with ritonavir. *Pharmacogenet Genomics* **20**:217-230.
13. **Hartkoorn RC, Kwan WS, Shallcross V, Chaikan A, Liptrott N, Egan D, Sora ES, James CE, Gibbons S, Bray PG, Back DJ, Khoo SH, Owen A.** 2010. HIV protease inhibitors are substrates for OATP1A2, OATP1B1 and OATP1B3 and lopinavir plasma concentrations are influenced by SLCO1B1 polymorphisms. *Pharmacogenet Genomics* **20**:112-120.
14. **Kalliokoski A, Niemi M.** 2009. Impact of OATP transporters on pharmacokinetics. *Br J Pharmacol* **158**:693-705.

15. **Nies AT, Niemi M, Burk O, Winter S, Zanger UM, Stieger B, Schwab M, Schaeffeler E.** 2013. Genetics is a major determinant of expression of the human hepatic uptake transporter OATP1B1, but not of OATP1B3 and OATP2B1. *Genome Med* **5**:1.
16. **Pasanen MK, Neuvonen PJ, Niemi M.** 2008. Global analysis of genetic variation in SLCO1B1. *Pharmacogenomics* **9**:19-33.
17. **Division of Microbiology and Infectious Diseases (DMID).** 2007. Adult Toxicity Table. November 2007 draft.
<http://www.niaid.nih.gov/LabsAndResources/resources/DMIDClinRsrch/pages/pharma.aspx> (last accessed 27 July 2014).
18. **Moultrie H, McIlleron H, Sawry S, Kellermann T, Wiesner L, Kindra G, Gous H, Van Rie A.** 2015. Pharmacokinetics and safety of rifabutin in young HIV-infected children receiving rifabutin and lopinavir/ritonavir. *J Antimicrob Chemother* **70**:543-549.
19. **Beal S, Sheiner LB, Boeckmann A, Bauer RJ.** 2009. NONMEM User's Guides. (1989-2009), v7. Icon Development Solutions, Ellicott City, MD, USA.
20. **Holford NH.** 1996. A size standard for pharmacokinetics. *Clin Pharmacokinet* **30**:329-332.
21. **Giacomini KM, Balimane PV, Cho SK, Eadon M, Edeki T, Hillgren KM, Huang SM, Sugiyama Y, Weitz D, Wen Y, Xia CQ, Yee SW, Zimdahl H, Niemi M, International Transporter C.** 2013. International Transporter Consortium commentary on clinically important transporter polymorphisms. *Clin Pharmacol Ther* **94**:23-26.
22. **Annaert P, Ye ZW, Stieger B, Augustijns P.** 2010. Interaction of HIV protease inhibitors with OATP1B1, 1B3, and 2B1. *Xenobiotica* **40**:163-176.
23. **Durnin JV, Womersley J.** 1974. Body fat assessed from total body density and its estimation from skinfold thickness: measurements on 481 men and women aged from 16 to 72 years. *Br J Nutr* **32**:77-97.
24. **Janmahasatian S, Duffull SB, Ash S, Ward LC, Byrne NM, Green B.** 2005. Quantification of lean bodyweight. *Clin Pharmacokinet* **44**:1051-1065.
25. **Lindbom L, Pihlgren P, Jonsson EN.** 2005. PsN-Toolkit--a collection of computer intensive statistical methods for non-linear mixed effect modeling using NONMEM. *Comput Methods Programs Biomed* **79**:241-257.

Supplemental Material

Detailed methods used to detect single nucleotide polymorphisms (SNPs):

Total Genomic DNA was isolated using the QIAamp DNA mini kit according to manufacturer's instructions. Purity was assessed following extraction by comparing the A260 and A280 ratio. DNA was normalised to 20ng/μl. Genotyping for *SLCO1B1* rs4149032, rs2306283, rs4149056 and rs11045819 was performed by real-time PCR allelic discrimination by standard methodology (95°C for 15 min, then 40 cycles of 95°C for 15 sec and 60°C for 1 min). The Applied Biosystems assay IDs for the first three SNPs were C_1901709_10, C_1901697_20 and C_30633906_10, respectively. For rs11045819, the forward primer, reverse primer, VIC probe and FAM probe were 5'CAGTGATGTTCTTACAGTTACAGGTATTCTAA3', 5'GAAGACTTTTTACTGTCAATATTAATTCTTACCTTTTCC3', 5'-ACTATCTCAGGTGATGCT-VIC, and 5'-CACTATCTCAGTTGATGCT-FAM, respectively.

Detailed population modeling methods

Data was analysed using NONMEM (version 7.1.2)(19) and PSN v.3.4.2.(25). Population pharmacokinetic parameter estimates, between-subject variability modelled exponentially, and residual variability were obtained with the first-order estimation method with interaction (FOCE+I). The objective function value (OFV), 'goodness-of-fit' plots and visual predictive checks were used to evaluate and guide model building, a bootstrap (n=200) was performed for model validation. Proportional, additive and combined residual error models were tested separately for rifabutin and 25-desacetyl rifabutin. Nested models were hypothesis-tested using the

likelihood ratio test in which the change in OFV approximates the X^2 distribution ($X^2_{1,0.05} > 3.84$). Non-nested models were compared using the Akaike information criterion (AIC).

Table S1: Expected mean±SD area under the concentration–time curve over 24 h (AUC_{0–24}) for rifabutin and des-rifabutin (AUCM_{0–24}) for specific subpopulations based on 500 simulations from the final model.

	<i>Female</i>	<i>Male</i>	<i>Carrier</i>	<i>Non-Carrier</i>	<i>Female Carrier</i>	<i>Male Carrier</i>	<i>Female non-Carrier</i>	<i>Male non-Carrier</i>
AUC _{0–24} (ng.h/L)	2830.4±160.2	2607.2±145.2	3050.4±187.3	2646.9±147.2	3142.9±176.8	2989.3±152.4	2788.1±153.6	2559.3±141.3
p-value	< 0.001		< 0.001		0.015 < 0.001 [#]		< 0.001 < 0.001 [†]	
AUCM _{0–24} (ng.h/L)	277.1±18.9	272.3±19.3	327.8±26.6	267.1±19.2	328.5±25.4	327.2±29.2	270.3±17.5	265.3±19.2
p-value	0.032		< 0.001		0.70 < 0.001 [#]		0.035 < 0.001 [†]	

[#] comparing female heterozygous carriers of *SLCO1B1* rs1104581 versus female non-carriers, [†] comparing male heterozygous carriers of

SLCO1B1 rs1104581 versus male non-carriers

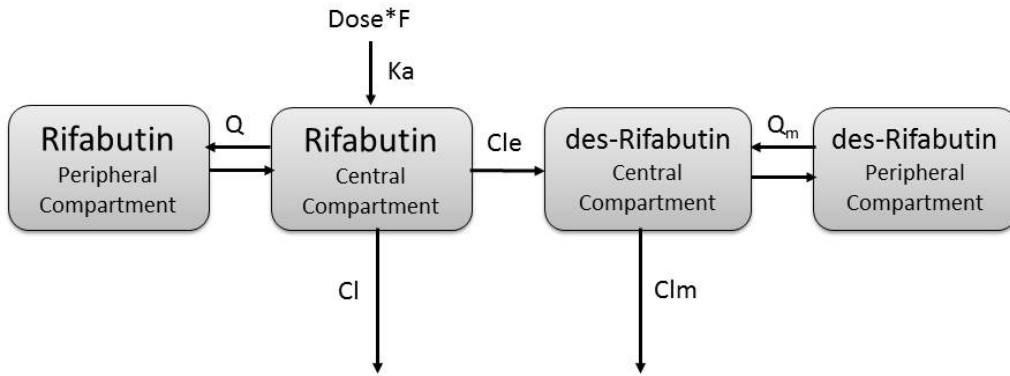


FIG S1. Structural model for rifabutin and 25-desacetyl rifabutin (des-Rifabutin).

F- bioavailability, ka- first order absorption rate constant, Q- intercompartmental clearance for rifabutin, Q_m - intercompartmental clearance for des-rifabutin, Cl-clearance of rifabutin, Cl_e - clearance of rifabutin to des-rifabutin, Cl_m - clearance of des-rifabutin

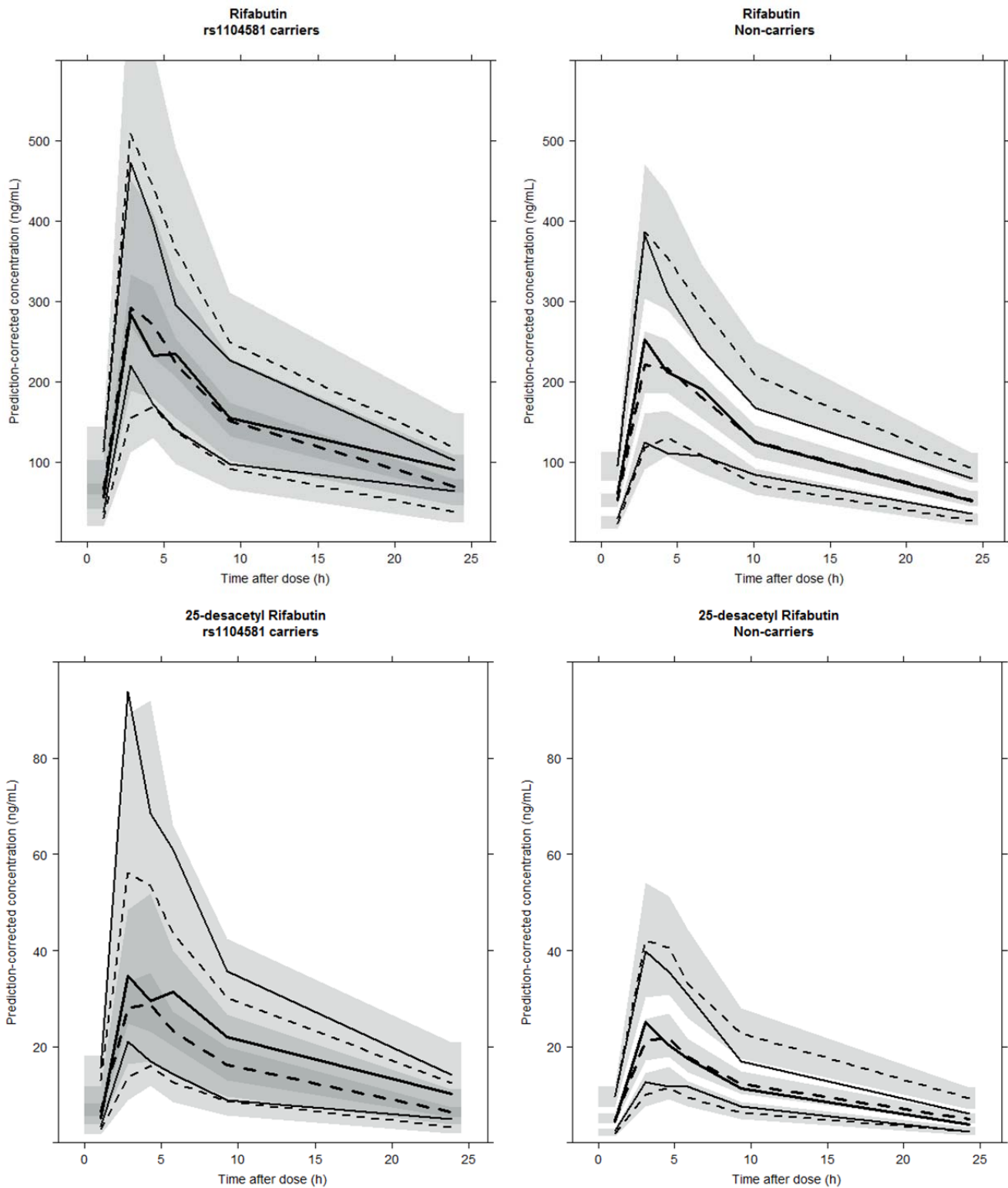
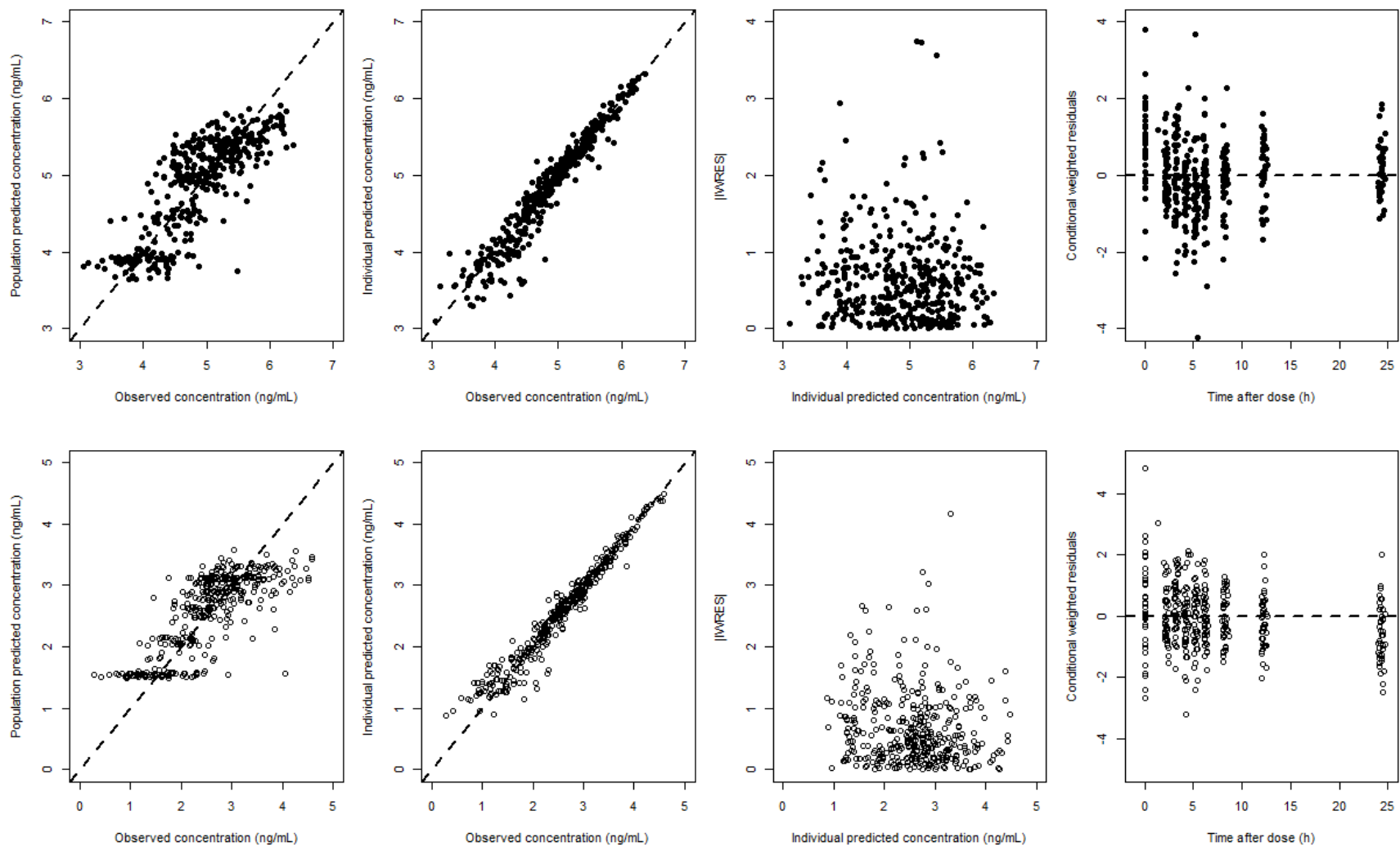


FIG S2. Prediction-corrected visual predictive check of the final model for rifabutin (top) and des-rifabutin (bottom) separated for rs1104581 carriers (left) and non-carriers (right). The solid upper, middle and lower lines represent the 90th, 50th and 10th percentile of the patients' observations. The dashed upper, middle and lower lines represents 90th, 50th and 10th percentile of simulated data. The grey shaded areas are the simulated confidence intervals for the corresponding percentiles.



1

2

FIG S3. Goodness-of-fit plots for rifabutin (closed circles, top row) and des-rifabutin (open circles, bottom row) for the final model.